

Generating sinusoidal flow surges in a large closed-loop wind tunnel

Nicholas Kay¹, Rory Buchanan², Peter Richards¹, Karl Stol¹

¹ *The University of Auckland, Auckland, 1010, New Zealand, nicholas.kay@auckland.ac.nz*

² *Cropsy Technologies, Auckland, 1010, New Zealand*

SUMMARY

To study the impact of gusts on drones, active flow control is required inside a wind tunnel for generating large-scale gusts representative of atmospheric conditions. Sinusoidal flow surge cycles are produced via a louvre-type rig in a large, closed-loop wind tunnel, to isolate the effects of frequency on the model under test. It is observed that the surge amplitude decreases with increasing louvre actuation frequency and a decrease in blockage. A lower amplitude is often associated with a lower surge quality due to the reduced signal, but high blockages also distort the sine wave to a triangular form, due to a slower flow acceleration as the louvres open. In all cases the primary signal is at the louvre frequency. The louvres-open wind speed has lesser impact on the surge amplitude than the blockage and frequency.

Keywords: Wind Tunnel, Experimental Methods, Flow Surge

1. INTRODUCTION

Wind tunnel tests of atmospheric flows face difficulties in generating large-scale, low frequency disturbances (Yang et al, 2020). This is particularly true for large-scale or full-size tests, such as on small drones or bridges. As such, active flow control methods are a useful tool, but can be expensive to manufacture and calibrate. Louvre-type rigs are simpler than fully-actuated grids (Makita and Sassa, 1991) or multi-fan arrays (Cao et al, 2002), and use rotating plates across the full width of the test area either to produce a transverse gust (by locally rotating the flow) or a longitudinal flow surge (via varying the blockage). For the latter, the louvres are often mounted downstream of the test area in an open-loop tunnel to reduce the effect of separated wake and harmonics impinging on the model (Greenblatt, 2016). This paper details the installation of a removable louvre-type rig for surging flow in a large closed-loop wind tunnel, to produce a sinusoidally-varying flow for at discrete frequencies and a range of surge amplitudes.

2. METHODOLOGY

The University of Auckland Boundary Layer Wind Tunnel is a closed-loop tunnel with a test section 3.6 m wide, 2.5 m tall and 24 m long. The surging flow rig developed employs vertically-pivoted louvres located halfway along this length, with no permanent disruption to the internal flow of the test section. The region of interest for this test is located between the upstream doors and the louvres, as shown in Fig. 1 as the blue rectangle. All data presented subsequently are from

the centre of this test area ($x = 1.5$ m, $y = 0$ m, $z = 1.25$ m). The louvres rotate in unison between angles (α) of 0° and 90° , motion provided by a Teknic Clearpath servo motor (6400 counts per revolution). To relieve pressure build-up, the doors upstream and downstream of the rig are left open throughout testing. Venting downstream has also been noted to improve wind tunnel gust response (Rennie et al, 2019), but the effects of upstream vents have not been explored prior.

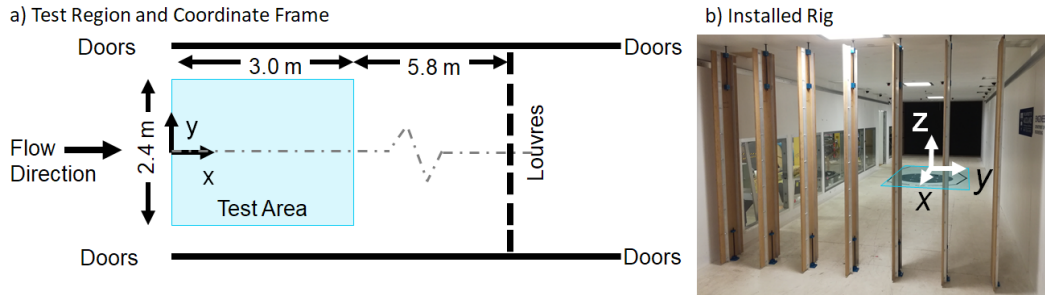


Figure 1. Surging flow rig installation in wind tunnel and coordinate frames

To produce a sinusoidal flow, the louvres were rotated sinusoidally for 15 cycles with varying frequencies and amplitudes, as listed in Table 1. In all cases, the louvres started at $\alpha = 0^\circ$. Transient velocities, u , were recorded with a TFI Cobra Probe Series 100 (Tfi, 2015) and synchronised with the louvre angle. Following the removal of the first three cycles to allow transients to pass, the time-averaged velocity within the steady cycles, U_1 , was found. The average peak deviation from this, representing the surge amplitude, u'_{max} , was subsequently assessed. The latter is used to assess the amplitude of the surge, taking the idealised form in Eq. (1). The timeseries data was compared to the idealised sinusoid to find the associated R^2 , as a measure of the quality of the sine wave.

Table 1. Flow conditions tested

Louvres-open wind speed, U_0 (m s^{-1})	4, 6, 8
Maximum louvre angle, α_{max} ($^\circ$)	15, 30, 45, 60, 75, 90
Maximum louvre blockage, β_{max} (%)	23, 39, 54, 65, 72, 74
Louvre cycle frequency, f (Hz)	0.05, 0.1, 0.25, 0.5, 0.75, 1.0

$$u = U_1 + u'_{max} \times \sin(2\pi ft) \quad (1)$$

4. RESULTS

Fig. 2a, presenting data for $U_0 = 6$ m s^{-1} , shows that the sinusoidal amplitude is highly-dependent on both frequency and maximum blockage. The maximum normalised amplitude of $u'_{max}/U_1 = 0.41$ occurs with the highest blockage and lowest frequency, dropping to $u'_{max}/U_1 = 0.01$ at the highest frequency and lowest blockage. The dependence on blockage declines as the frequency increases, with all cases below $\beta_{max} = 55\%$ producing $u'_{max}/U_1 < 0.05$ at 1 Hz. This decline in amplitude is to be expected, as large wind tunnels typically have a bandwidth of less than 1 Hz (Greenblatt, 2016). However, as most turbulent energy is expected below 1 Hz (Berman, 1965), this limitation is acceptable. As u'_{max}/U_1 declines, Fig 2b shows a corresponding reduction in R^2 . This is likely a function of the signal-to-noise ratio, with a greater amplitude producing a more defined signal at the specified frequency. However, the slight reduction in R^2 for a given frequency when $\beta_{max} = 74\%$ suggests that distortion may occur at higher blockages.

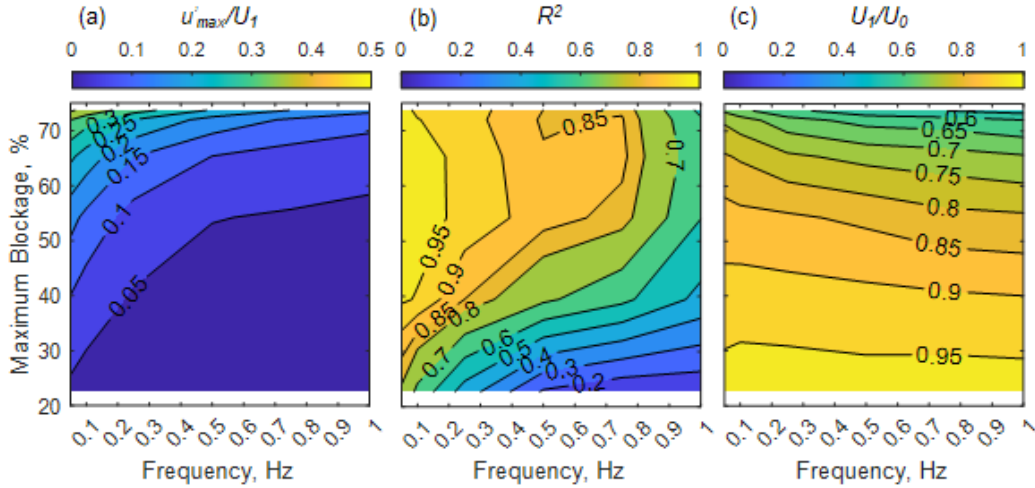


Figure 2. (a) surge amplitude, (b) R^2 for $U_0 = 6 \text{ m s}^{-1}$ and (c) mean velocity

The amplitudes in Fig. 2 are normalised by U_1 , rather than the louvres-open speed, U_0 , as the former is shown in Fig. 2c to not be consistent. In particular, increasing blockage decreases U_1 . A decrease in U_1 is also seen with increasing frequency, albeit to a lesser extent than the variation with blockage. Fig 3, which presents the phase averaged transient velocity for four frequencies and two β_{max} , shows that increasing the blockage reduces both the maximum and minimum velocities seen in a given cycle, thereby reducing U_1 . Increasing frequency, on the other hand, has a greater effect on reducing the maximum velocity than changes in the minimum, resulting in less change to U_1 , but continuing to decrease u'_{max}/U_1 .

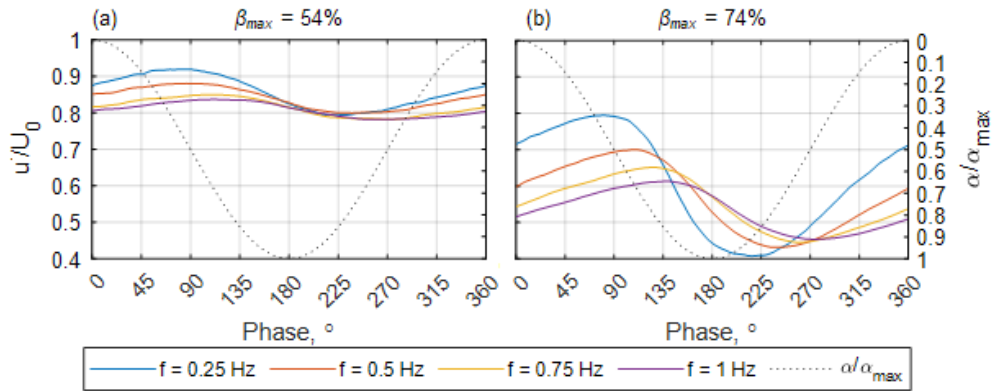


Figure 3. Phase-averaged velocity for (a) $\beta_{max} = 54\%$ and (b) $\beta_{max} = 74\%$

Fig. 3 also shows that the maximum velocity occurs later in the cycle relative to the louvres fully-opening than the minimum velocity compared to the louvres fully-closing, resulting in a skewed sinusoid. This is clearest in Fig 3b, but can also be seen to occur with increasing frequency in Fig 3a. The louvres are more effective at slowing the flow, which can divert out the open doors, than the fans are at re-establishing it through the test area. Active shutters over the doors may improve this response (Cook et al, 2020). This skew likely contributes to the slight reduction in R^2 seen in Fig 2b at the highest β_{max} . However, as the velocity signal repeats over the same period as the louvre cycle, the signal strength at the desired frequency is high.

Fig.4 shows u'_{max}/U_1 does increase slightly with an increase in U_0 , the greater fan pressure likely aiding the acceleration from minimum speed. However, this is a lesser contributor relative to the frequency and maximum blockage.

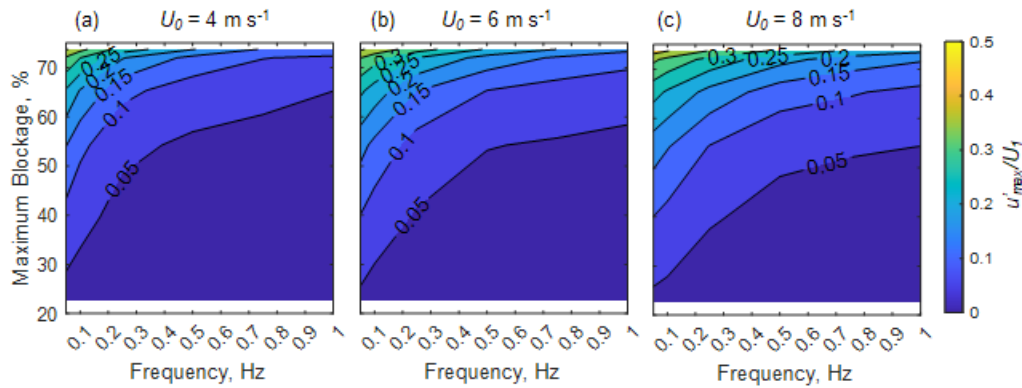


Figure 4. Surge amplitude at (a) $U_0 = 4 \text{ m s}^{-1}$, (b) $U_0 = 6 \text{ m s}^{-1}$ and (c) $U_0 = 8 \text{ m s}^{-1}$

7. CONCLUSIONS

A surging flow rig has been retrofitted to a closed-loop wind tunnel for producing repeating sinusoidal flow surges, with the purpose of testing the full-size drones to atmospheric-scale flows. The amplitude of the surge is seen to be highly dependent on the blockage and frequency, but less so the louvres-open speed. The cycle distorts from the desired sinusoid at high frequencies and blockages, due to slow acceleration as the louvres open, which may be improved by active venting upstream.

ACKNOWLEDGEMENTS

The research reported in this article was conducted as part of “Enabling unmanned aerial vehicles (drones) to use tools in complex dynamic environments UOCX2104”, which is funded by the New Zealand Ministry of Business, Innovation and Employment.

REFERENCES

- Berman, S., 1965. Estimating the longitudinal wind spectrum near the ground. Quarterly Journal of the Royal Meteorological Society 91, 302-317.
- Cao, S., Nishi, A., Kikugawa, H., Matsuda, Y., 2002. Reproduction of wind velocity history in a multiple fan wind tunnel. Journal of wind engineering and industrial aerodynamics 90, 1719-1729.
- Cook, T., Gunasekaran, S., Ol, M.V., Mongin, M.P., 2020. Frequency Response of a Shuttered Open Jet Wind Tunnel, AIAA Scitech 2020 Forum, Orlando, FL, USA, p. 1760.
- Greenblatt, D., 2016. Unsteady low-speed wind tunnels. AIAA Journal 54, 1817-1830.
- Makita, H., Sassa, K., 1991. Active turbulence generation in a laboratory wind tunnel, in: Johansson, A.V., Alfredsson, P.H. (Eds.), Advances in Turbulence 3. Springer, pp. 497-505.
- Rennie, M.R., Catron, B., Zubair Feroz, M., Williams, D., He, X., 2019. Dynamic behavior and gust simulation in an unsteady flow wind tunnel. AIAA Journal 57, 1423-1433.
- Tfi, 2015. Cobra Probe. Turbulent Flow Instrumentation.
- Yang, B., Zhang, B., Zhou, X., Ren, Y., Zhang, Y., 2020. Artificial simulation of complex unsteady wind in an ABL wind tunnel with dual axial fans. Journal of Wind Engineering and Industrial Aerodynamics 197, 104075.